Article

A new super-efficiently flame-retardant bioplastic-poly (lactic acid): flammability, thermal decomposition behavior and tensile properties

xiaomin zhao, Francisco Reyes Guerrero, Javier Llorca, and DeYi Wang

ACS Sustainable Chem. Eng., **Just Accepted Manuscript** • DOI: 10.1021/acssuschemeng.5b00980 • Publication Date (Web): 24 Nov 2015

A new super-efficiently flame-retardant bioplastic-poly (lactic acid): flammability, thermal decomposition behavior and tensile properties

Xiaomin Zhao[1,2], Francisco Reyes Guerrero[1], Javier Llorca[1,2], De-Yi Wang[1]*

[1]IMDEA Materials Institute, C/Eric Kandel, 2, 28906 Getafe, Madrid, Spain

[2]Technical University of Madrid (UPM), 28006, Madrid, Spain

Corresponding author: De-Yi Wang: Tel.: +34-917871888, *E-mail address*: deyi.wang@imdea.org

Abstract

In this study, a super-efficiently flame-retardant bioplastic-poly (lactic acid)-was developed by incorporating gas-solid biphase flame retardant, N, N'-Diallyl-P-phenylphosphonicdiamide (P-AA), into PLA matrix. The flame retardancy of PLA/P-AA was investigated by limiting oxygen index (LOI), vertical burning test (UL94) and cone calorimeter test. Surprisingly, it was noted that only 0.5 wt% loading of P-AA increased LOI value of PLA from 20.5 to 28.4 and passed UL 94 V-0 rating at 3.2 mm thickness. In order to understand the effect of P-AA on thermal decomposition behavior of PLA, a comprehensive study was investigated in this paper, including (i) adopting modified Coats-Redfern method to study the thermal decomposition kinetics of PLA and PLA/P-AA systems; (ii) characterizing the evolved gaseous products and the residues in the condense phase by thermogravimetry linked Fourier transform infrared spectroscopy (TGA–FTIR) and variable temperatures Fourier transform infrared spectroscopy (VT-FTIR) techniques, respectively. Moreover, tensile properties of PLA and PLA/P-AA were studied.

Keywords: Bioplastic; Poly (lactic acid); Flame retardancy; Thermal degradation behaviors; TGA-FTIR.

Introduction

As one promising bio-based polymer, the development of poly (lactic acid) (PLA) presents diversified. At first, PLA applications was focused on biodegradable applications, such as medical, agriculture, engineering, compostable products, and packaging materials. Nowadays, PLA is introduced into many new fields such as electronic appliances, automotive materials, textile and transportation.[1-2] For these burgeoning applications, flammability of PLA is one of challenge to be solved on account of health and environment issues. [3-4]

Researchers have attempted many methods to improve flame retardancy of PLA in the last years. [3-9] Especially, nano-inorganic, phosphorous-based and intumescent flame retardants had been used as flame-retardant additives for PLA and some new effective flame-retardant systems had been developed as well. [10-19] Grégory Stoclet et al. reported that 17wt% halloysite decreased the peak of heat release rate (pHRR) of PLA matrix by 40 wt% compared with PLA control.[15] Lei Song et al. found the synergistic effect between intumescent flame retardant (pentaerythritol phosphate (PEPA) and melamine phosphate (MP)) and polyhedral oligomeric silsesquioxanes (POSS) on PLA matrix. 25 wt% of IFR only led PLA to V-1 rating while 20 wt% of IFR plus 5wt% of POSS led to UL94 V-0 rating.[16] However, these high loadings of flame retardants would scarify thermal or mechanical properties. Hence, aiming to keep the balance between the flame retardancy and other properties of PLA, development of high efficient flame retardancy for PLA has been regarded as an effective approach. For example, Ping Wei et al. applied expandable graphite intercalated with sulphuric acid (GR) into PLA matrix and found that 5 wt% loading of such additives was enough to lead PLA pass V-0 rating.[17] Qian Yong et al. reported that only 0.5 wt% incorporation of mesoporous flame retardant (Al-SBA-15) made PLA matrix pass V-0 rating along with 30 wt% of LOI value. [18] Wang et al. synthesized successfully flame-retardant PPLA via the chain-extending reactions of dihydroxyl terminated pre-poly (lactic acid) using ethyl phosphorodichloridate as chain extender. Only 5 wt% of PPLA endowed PLA to get LOI value of 25 and UL-94 V-0 rating. [19]

The aim of this work was to develop super-efficiently flame-retardant PLA system, keep the balance of flame retardancy and thermal/mechanical properties, and understand

its thermal decomposition behavior at the same time. Following this idea, in this paper the flame retardant, N, N'-Diallyl-P-phenylphosphonicdiamide (P-AA) was applied into PLA matrix to prepare a novel flame-retardant PLA composites (PLA/P-AA). Limiting oxygen index (LOI), UL 94 test and cone calorimeter test were used to characterize the flame retardancy of PLA and PLA/P-AA systems. A comprehensive study was done to investigate the effect of P-AA on the thermal decomposition behavior of PLA. It included: (i) a modified Coats-Redfern method was adopted to study the thermal decomposition kinetics of PLA and PLA/P-AA systems; (ii) the evolved gaseous products and the residues in the condense phase were characterized by thermogravimetry-fourier transform infrared spectroscopy (TGA–FTIR) and variable temperatures Fourier transform infrared spectroscopy (VT-FTIR) techniques respectively. In addition, the mechanical properties of PLA and PLA/P-AA were investigated via tensile test.

Experiments

Materials

Phenylphosphonic dichloride (PPDCl, 90%), Phenyl dichlorophosphate(95%), allylamine (98%), diethyl ether, diethyl ether and triethylamine (TEA) were purchased from Sigma-Aldrich Corporation and used without any further purification. Poly (lactic acid) (PLA, 2003D) was purchased from NatureWorks LLC in American.

Synthesis of N, N'-Diallyl-P-phenylphosphonicdiamide (P-AA) [20]

The synthesis rout of P-AA was described in Scheme 1. In detail, Allylamine (AA) (0.21 mol) dissolved in diethyl ether (100 ml) together with triethylamine (TEA, 0.2 mol) at 0-5 ^{o}C in three-neck flask. Then into the flask dropped wise PPDCl (0.1 mol) which solve in 100 mL diethyl ether. The temperature kept for 2 h at 0-5 °C and then the mixture continued to react at room temperature for 5h. The generated triethylamine hydrochloride salts filtrated off. The raw product was separated from the filter liquor after reduced pressure distillation. The product P-AA finally was obtained after washing the raw product by water for three times. P-AA: m.p. 67 °C; white solid; yield, 80wt%; ^{1}H-NMR (DMSO-d_6): δ(ppm), 7.8-7.4 (Ar-H, 5H); 5.8 (=CH, 2H); 5.1- 4.9 (=CH_2, 4H); 3.4 (-CH_2-, 4H); ^{13}C-NMR (DMSO-d_6): δ (ppm), 137.8, 135.5, 134.3, 131.2, 130.6, 127.8, 114.2,

42.4; ^{13}P-NMR (DMSO-d_6): δ (ppm), 19.8. FTIR spectra: KBr, 3200 cm^{-1} (-NH-), 3057, 1450, 741and 693 cm^{-1} (Ph), 3008 cm^{-1} (C=C-H), 2890 cm^{-1} (-CH_2-), 1643 cm^{-1}(C=C), 1180 cm^{-1} (P=O), 1012 cm^{-1} (P-N-C). The spectra of NMR and FTIR were collected as Figure S1-S4 in Supporting Information.

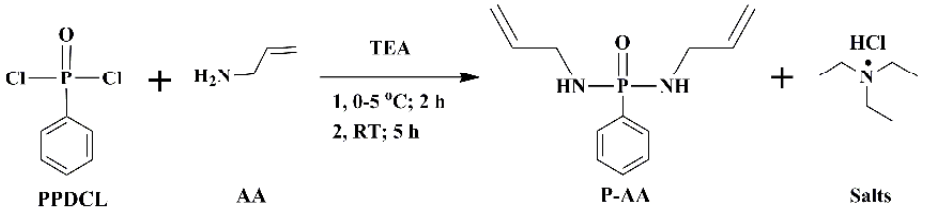

Scheme 1 The synthesis rout of flame retardant P-AA

Preparation of PLA and PLA/P-AA composites

The preparations of all samples were followed two steps: extrusion-pelletization and hot compression molding. For example, the procedure of PLA/P-AA composites was as following. First, a twin-screw extruder machine (KETSE 20/40 EC, Brabender) was used to mix PLA matrix with P-AA. PLA and P-AA were dried at 70 °C for 12 h before used. The parameter setting was: screw speed, 50 rpm; temperature control, zone 1(160 °C), zone 2 (165 °C), zone 3(165 °C), zone 4 (170 °C), nose (165 °C). Then the mixture particles were pressed with different sample modules in a hot presser at 160 °C for 3 minutes. In comparison, the specimens of PLA control were prepared by the same procedure.

Characterization

The oxygen index meter (FTT, UK) was used to measure the LOI of PLA, PLA/P-AA composites with sheet dimension of 130×6.5×3 mm^3 according to ASTM D2863-97. Vertical burning test was carried on UL 94 Vertical Flame Chamber (FTT, UK) with sheet dimension of 130×13×3.2 mm^3 and/or 130×13×1.6 mm^3 according to ASTM D3801. Five specimens were tested for each composition. The surface temperature (ST) of PLA and PLA/P-AA (0.5 wt%) was collected by infrared thermometer (IR thermometer) during the UL 94 test. The emissivity for IR thermometer was always set as 0.950 for IR thermometer. Cone colorimeter tests were carried out according to the ISO 5660-1 standard with a cone calorimeter (FTT). Square specimens (100×100×4 mm^3) were

irradiated at a heat flux of 35 kW/m^2. Two samples at lease were tested for each composition. The thermal decomposition properties were characterized by the thermal gravimetric analyzer (TA Q50, USA). The sample amounts were in range of 8-10 mg and the heating procedure was: 10 ^{o}C /min heating from room temperature to 600 ^{o}C. Multiple heating rates (β) (10, 20 30, 40 ^{o}C /min) were done for TGA analysis in order to study thermal decomposition kinetics of PLA and PLA/P-AA composite. The evolved gaseous products from PLA and PLA/ P-AA (1 wt%) were characterized by coupling techniques of thermogravimetry (TA, Q50) coupled with Fourier transform infrared spectroscopy (Nicolet iS50) (TGA–FTIR). The test procedure for TGA was 10 ^{o}C/min from room temperature to 600 ^{o}C under nitrogen atmosphere. The evolved gaseous products went through stainless steel line into the gas cell under nitrogen carrier gas for FTIR detection. FTIR spectra recorded in a range of 4000–500 cm^{-1} with a 4 cm^{-1} resolution and averaging 8 scans. Variable temperatures FTIR spectra (VT-FTIR) were collected under a heating device coupling accessory. The heating ramp was 10 ^{o}C/min to 400 ^{o}C. The scanning range for FTIR spectra is 4000-500 cm^{-1} with a resolution of 4 cm^{-1}. The sample is scanned 16 times and the sampling interval was 15.58 s. Tensile test was performed on universal electromechanical testing machine (INSTRON 3384, MA, and USA) according to standard ASTM D 638 at room temperature. The crosshead speed was set to 3 mm/min and five specimens were tested for each composition.

Results and discussion

Flammability

In this segment, the effect of P-AA on flammability of PLA was studied by two bench-scale fire tests: limiting oxygen index (LOI) and UL 94 vertical burning test. Tab. 1 listed the LOI and UL 94 results (3.2 mm and/or 1.6 mm) for PLA and PLA/P-AA systems. The UL 94 test videos of PLA, PLA/P-AA (0.5 wt%) and PLA/P-AA (1 wt%) were added as Supporting Information (Video). Moreover, the surface temperature (ST) was monitored by IR thermometer during UL 94 test. Fig. 1 A) showed the screenshots from UL 94 test videos with different loading samples; B) described the curves of ST of PLA and PLA/P-AA (0.5 wt%) against testing time. From Tab. 1, it showed that LOI value of PLA control was only 20.5 and no rating in UL94 test. However, the addition of P-AA obviously reduced the flammability of PLA. First of all, LOI of flame rertardant PLA

increased along with the rising of P-AA loading. For example, the LOI value of PLA/P-AA (0.3 wt%) was 24% in comparison with PLA control; as the loading of P-AA rose to 2 wt%, LOI value of PLA/P-AA (2 wt%) was increased to 32.5 %. Furthermore, the addition of P-AA induced great impact on the vertical burning behaviors of PLA in UL 94 test. With thickness of both 3.2 and 1.6 mm, PLA control burnt to the clamp along with fast and burning dripping (shown in Fig. 1A). However, by incorporating flame retardant P-AA into PLA matrix, very surprised phenomena were appeared, showing that only 0.3 wt% loading of P-AA endowed PLA matrix to pass UL 94 V-0 rating at 3.2 mm thickness. When P-AA loading was 0.5 wt%, PLA/P-AA (0.5 wt%) passed V-2 rating at 1.6 mm thickness, while passed V-0 rating at 3.2 mm thickness. Moreover, there was almost no flame observed during the whole ignition of PLA/P-AA (0.5 wt%) which was shown in Fig. 1A. Meanwhile, its dripping behavior was much slower than that of PLA control. Even for thinner sample (1.6 mm), 1 wt% of P-AA into PLA was enough to pass UL94 V-0 rating. As a whole, P-AA exhibited super efficiency on reducing the flammability which was illustrated by the increase of oxygen sensitivity and the given self-extinguishment ability of PLA matrix.

Tab. 1 LOI and UL 94 results of PLA and PLA/P-AA composites

Sample	LOI (%)	UL 94	
		1.6 mm	3.2 mm
PLA Control	20.5	No rating	No rating
PLA/P-AA (0.1 wt%)	22.9	No rating	Na rating
PLA/P-AA (0.3 wt%)	25.5	No rating	V-0
PLA/P-AA (0.5 wt%)	28.4	V-2	V-0
PLA/P-AA (1 wt%)	29.6	V-0	V-0
PLA/P-AA (2 wt%)	32.5	V-0	V-0

Aiming to understand more about this fire behavior, during UL 94 test the temperature of samples' surface was studied by IR thermometer. In Fig. 1 B), ST of PLA control continuously increased during the whole ignition (10s in total). Then the value almost stabilized at around 380 ^{o}C after the ignition due to the continuously burning. However, a special phenomenon was observed in PLA/P-AA system that ST of PLA/P-AA (0.5 wt%) first increased around to 300 ^{o}C until 5-7 s, afterwards the temperature started decreasing

in the following 5-3 s. This result was repeatable more than 3 times and was provable. For the 2nd ignition, ST of PLA/P-AA increased to 350 ^{o}C, and then decreased immediately due to the self-extinguish. Regarding to the reason, it's explained by the flame inhibition effect of P-AA on PLA matrix. Once the flame touched the PLA matrix, the decomposition of PLA started and the gas products produced continues flame for PLA reference, which made the temperature of PLA surface increased continually. However, the gas products of PLA/P-AA (0.5 wt%) had no chance to form flame reaction cycle due to the inhibition effect of PO· radicals from the decomposition of P-AA. Hence, the heat from the testing flame increased ST of PLA/P-AA (0.5 wt%) in one side; supported the melt and decomposition of PLA matrix in another side. When the melt and decomposition occupy the main consumption of heat from testing flame, ST of PLA/P-AA (0.5 wt%) would decrease.

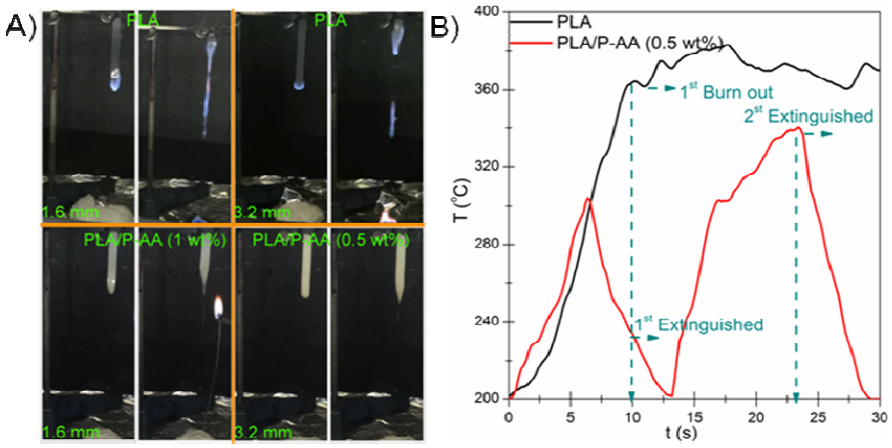

Fig. 1 A) The screenshots from UL 94 test videos of PLA with thickness 1.6 and 3.2 mm, PLA/P-AA (1 wt%) with thickness 1.6 mm and PLA/P-AA (0.5 wt%) with thickness 3.2 mm; B) the surface temperature monitored by IR thermometer vs time curves of PLA and PLA/P-AA (0.5 wt%) (3.2 mm)

Combustion behavior

Cone calorimeter (CONE) is one of widely used methods for flame-retardant polymer materials in recent twenty years. It measures heat release rate (HRR) by oxygen consumption calorimeter.[20] In this segment, CONE was used to study the combustion behavior of PLA and PLA/P-AA at 35 kW/m^2 heat flux. The characteristic curves of HRR vs time and mass vs time were shown in Fig. 2 A and B, respectively. Tab. 2 collected the main parameters: time to ignition (TTI), peak of heat release rate (pHRR),

and total heat release (THR), average effective heat of combustion (Avg. EHC), and total smoke release (TSR) from CONE for PLA and PLA/P-AA.

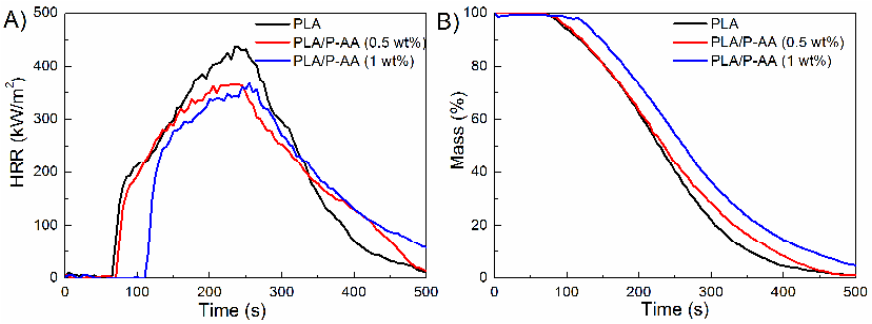

Fig. 2 A) HRR vs time curves of PLA and PLA/P-AA; B) mass curves of PLA and PLA/P-AA

TTI of PLA control was 66 s. When PLA was ignited, flame spread rapidly into the entire surface and its pHRR was 437 kW/m^2. In comparison, PLA/P-AA had lower pHRR and THR, showing pHRR decreased to 366 kW/m^2 when P-AA loading was 0.5 and/or 1 wt%. Furthermore, TTI of PLA /P-AA (1 wt%) was delayed to 111 s which was 45 s longer than that of PLA. Meantime, mass loss curves in Fig. 2B showed that the initial mass loss of PLA/P-AA (1 wt%) was also delayed significantly. The decrease of pHRR was attributed to the flame inhibition of P-AA which induced incomplete combustion behavior.[17] The delayed TTI showed that the introduction of P-AA improved the flash resistance of PLA. In addition, TSR increased for PLA/P-AA compared with PLA which might be due to the incomplete combustion behavior.

Tab. 2 CONE data for PLA and PLA/P-AA at 35 kW/m^2

Samples	TTI[a] (s)	pHRR[b] (kW/m^2)	THR[c] (MJ/m^2)	Avg. EHC[d] (MJ/kg)	TSR[e] m^2/m^2
PLA	66(±3)	437(±15)	96.3(±3.5)	17.7	39.3(±2)
PLA/PAA (0.5 wt%)	69(±2)	366(±10)	90.5(±2.9)	17.6	42.4(±4)
PLA/PAA (1 wt%)	111(±5)	366(±17)	87.2(±2.5)	17.1	46.5(±3)

a: TTI was time to ignition; b: pHRR was peak of heat release rate; c: THR was total heat release; d: Avg. EHC was the average effective heat of combustion; e: TSR was total smoke release.

The results of LOI, UL 94 and cone calorimeter tests showed that the addition of P-AA greatly impacted the flame retardancy of PLA in different aspects. Considering the lowing loading amount and the few residues after the cone calorimeter test, the main

mechanism of P-AA was proposed in the gas phase which meant the flame inhibition on PLA. From the previous report[20], P-AA produced PO· radicals when it decomposed at high temperature. This radical was able to annihilate H· and OH· radicals which were produced from the decomposition of PLA. Hence, the ignition conditions for PLA/P-AA were higher than that of PLA. The increase of LOI value, strong self-extinguishment phenomena in UL 94 test and low pHRR in cone calorimeter test were related to such effect.

Thermal decomposition behaviors of PLA and PLA/P-AA composites

In this section, the effect of P-AA on the thermal decomposition of PLA was studied by TGA analysis, TGA-FTIR and VT-FTIR techniques. Fig. 4 showed the TGA curves of PLA and PLA/P-AA systems. The thermal decomposition kinetics of PLA and PLA /P-AA (1 wt%) were investigated by means of Coats-Redfern (modified) method [21,22] according to the TGA of multiple heating rates. Fig. 4 (A), (B) listed the fitted curves of $\ln(\beta/T^2)$ against 1/T of PLA and PLA/P-AA (1 wt%) at different conversation (α). Tab. 3 collected the apparent activation energy (Ea) and the corresponding coefficients of determination (r^2) calculated from the fitted curves of $\ln(\beta/T^2)$ against 1/T at each α.

Thermal decomposition kinetics

From TGA curves of PLA and PLA/P-AA shown in Fig. 3, the addition of P-AA altered the thermal decomposition behavior of PLA in minor way under nitrogen atmosphere. As the loading of P-AA rose to 1 wt%, the initial decomposition temperature and the temperature at maximum decomposition rate decreased slightly. Besides, the residue kept at the same value (around 0.7 wt%) for both of PLA/P-AA(0.5 wt%) and PLA/P-AA(1 wt%) at 550 ^{o}C.

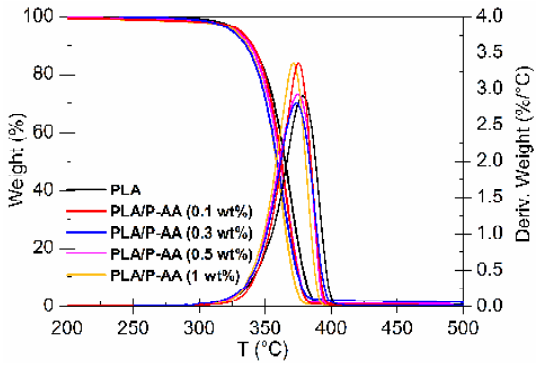

Fig. 3 TGA and DTG curves of PLA and PLA/P-AA composites

Moreover, the thermal decomposition kinetics of P-AA on PLA control was investigated by using the modified Coats-Redfern method (Burnham) [21,22] that was developed from the Coats and Redfern equation with a muti-heating rate application. In this study, the multi-heating rate was set as: 10, 20 30, 40 ^{o}C /min, respectively. A simple theory introduction about this method was described in the following. Generally, the typical equation to analyzing the thermal decomposition kinetics was described as following on basis of a dynamic TGA process:

$$\frac{d\alpha}{dT} = \frac{A}{\beta} e^{(-\frac{E}{RT})} f(\alpha) \qquad (1)$$

In this equation, β was set as heating rate during the test: $\beta = \frac{dT}{dt}$

The final expression for this iso-conversional method was described as:

$$\ln\left(\frac{\beta}{T^2(1-\frac{2RT}{E})}\right) = \ln\left(-\frac{AR}{E\ln(1-\alpha)}\right) - \frac{E}{RT} \qquad (2)$$

In this method, Ea was calculated from the fitted curves: ln (β/T^2) plotted against 1/T, which gave slope –Ea/R of line at different α. Through this relationship, the Ea values can be calculated using slopes obtained from each fitted curves for every degree of α. [21,22]

From Fig. 4(A, B), the fitted curves of ln (β/T^2) against 1/T almost were parallel at different α for PLA control. However, the slope of fitted curves continually increased for PLA/P-AA (1 wt%). Seen from the calculated Ea (Tab. 3), Ea showed the same decreasing trend for PLA and PLA/P-AA (1 wt%). The addition of P-AA reduced Ea of

PLA matrix no matter at low α or high α. What's more, PLA/P-AA (1 wt%) showed larger reduction with the riding of α. For example, as α was 0.9, Ea of PLA control decreased by 25 kJ/mol compared with that when α was 0.2. However, Ea of PLA /P-AA (1 wt%) decreased by 44 kJ/mol as α was 0.9 compared with that as α was 0.2. As a whole, the addition of P-AA decreased the thermal decomposition Ea of PLA matrix. At high α, this effect was stronger than that at low α, which meant that P-AA might change the decomposition rout of PLA. This change was considered to be attributed by the phosphonic acid produced by the thermal decomposition of P-AA.[20]

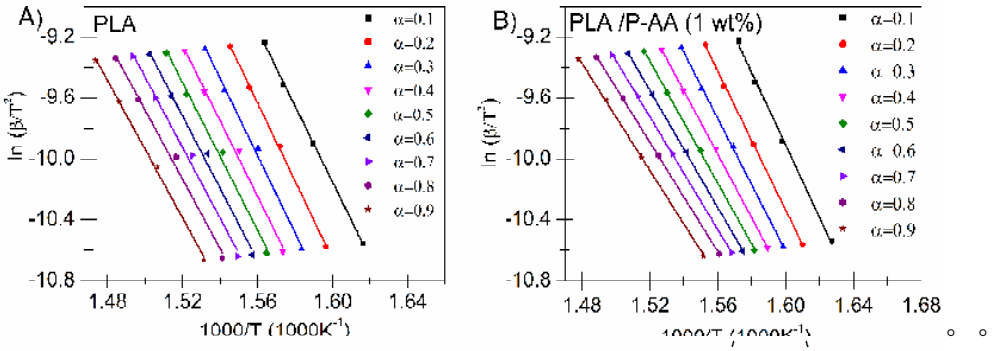

Fig. 4 A) The plot curves of ln (β/T^2) against 1/T of PLA at different α; B) The plot curves of ln (β/T^2) against 1/T of PLA/P-AA (1 wt%) at different α

Tab. 3 Calculated Ea and r^2 of PLA and PLA/P-AA (1 wt%) at different decomposition α

Conversation (α)	PLA		PLA /P-AA (1 wt%)	
	Ea (kJ/mol)	r^2	*Ea* (kJ/mol)	r^2
0.1	208	0.9995	198	0.9963
0.2	213	0.9983	190	0.9992
0.3	211	0.9948	181	0.9994
0.4	206	0.9925	173	0.9994
0.5	202	0.9914	166	0.9994
0.6	197	0.9911	160	0.9996
0.7	193	0.9908	154	0.9997
0.8	189	0.9905	149	0.9997
0.9	188	0.9974	146	0.9994

Characterization of evolved gaseous products via TGA-FTIR analysis

The evolved gaseous products were collected and identified by means of TGA-FTIR technique for the purpose of understanding the thermal decomposition behavior of PLA and PLA/P-AA (1wt%). Fig. 5 A) and B) listed the 3-D images of evolved gaseous products of PLA and PLA/P-AA (1 wt%) separately during TGA test; C) showed Gram-Schmidt curves vs temperature of these two systems. Fig. 6 showed the FTIR spectra of evolved gas products of PLA around 380 ^{o}C

Corresponding to the reported results [23], the main decomposition products of PLA were identified as lactide or cyclic oligomers (carbonyl compounds, 1780 cm^{-1}), hydrocarbons (2950 cm^{-1}), carbon monoxide (CO, 2181 and 2111 cm^{-1}), carbon dioxide (2358 cm^{-1}) and water (3577 cm^{-1}) in Fig. 6. The four peaks in finger print range were appointed as C-H stretching (1371 and 930 cm^{-1}) and C-O stretching (1244 and 1105 cm^{-1}). The total IR absorbance of evolved gaseous products for PLA and PLA/P-AA (1 wt%) was similar from Gram-Schmidt curves in Fig. 5 C), which indicated that the main decomposition products of PLA did not alter too much after adding low loading P-AA. However, there was an obvious peak loss as compared the 3-D images of TGA-FTIR results of PLA and PLA/P-AA (1 wt%). The IR absorbance of this peak (1244 cm^{-1}) against temperature was showed in Fig. 5 D). The intensity of peak 1244 cm^{-1} decreased in remarkable way after the addition of P-AA (1 wt%). The decrease of this peak was due to the radicals produced by the thermal decomposition of P-AA. [17] These products were considered to enable accelerate the radical reactions occurred at high temperature. In this case the amounts of ketone compounds would increase whereas the amounts of C-O bonds from ether compounds decreased.

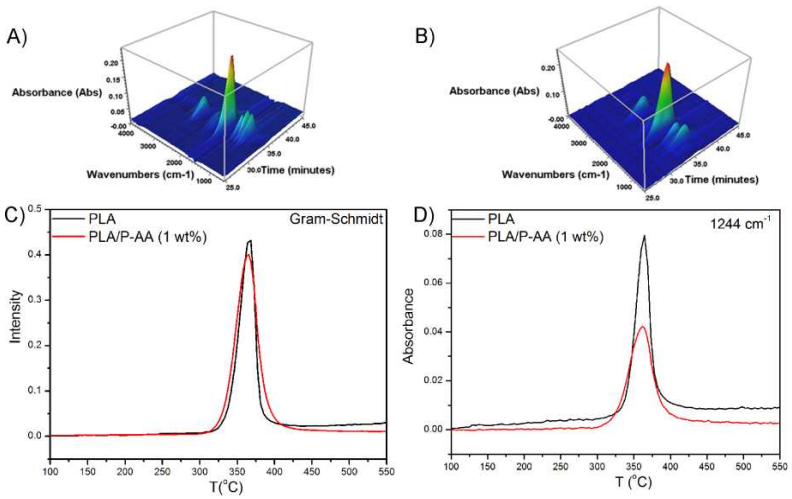

Fig.5 A) 3-D image of TGA-FTIR results of PLA; B) the 3-D image of TGA-FTIR results of PLA/P-AA (1 wt%); C) the Gram- Schmidt curves vs temperature of PLA and PLA/P-AA (1wt%); D) the absorbance at 1244 cm^{-1} vs temperature curves of PLA and PLA/P-AA (1wt%);

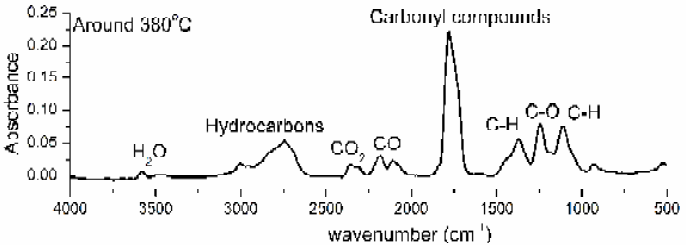

Fig. 6 FTIR spectra of evolved gas products of PLA around 380 °C

Solid phase characterization via VT-FTIR analysis

VT-FTIR analysis was used to investigate the difference in the solid phase during thermal decomposition. Fig. 7 described the FTIR spectra of solid phase at different temperatures for PLA (A) and PLA/P-AA (1 wt%) (B). Compared these two figures, it was hard to find new peaks caused by the addition of P-AA due to the low amount. Lactic acid was dominant in the condensed phase from the initial to the end of decomposition. The difference between the spectra of these two systems was summarized as two points at different temperatures: one was the intensity reduction of each peak was faster for PLA than that of PLA/P-AA (1 wt%); the other was the peak intensity around 3580 cm^{-1} which was appointed as –OH group from acyclic acid or acyclic oligomers was higher for PLA than that for PLA/P-AA (1wt%). In fact, the thermal degradation of PLA had been studied and reported by several groups such as McNeill and Leiper, Cam and Marucci,

Aoyagi et al. [1,24] Thermal degradation of PLA predominantly consisted of random main-chain scission and unzipping depolymerization reactions. The random degradation reaction involved hydrolysis, oxidative degradation, cis-elimination, and intramolecular and intermolecular transesterification. Here, in this work, intramolecular transesterification and cis-elimination were assumed to be the main reactions under oxygen-free condition. From the results of TGA-FTIR and VT-FTIR, it was proved that these reactions were not disappeared caused by the addition of P-AA. However, P-AA affected the thermal decomposition of PLA in some ways. For example, the acid products from the decomposition of P-AA was able to slow down the cis-elimination inside the condense phase, which meant that the amount of acid products was lower in PLA/P-AA system. Meanwhile, the weaker acid environment would decrease the transesterification rate. This speculation was able to explain the spectra intensity of PLA/P-AA (1 wt%) was higher than that of PLA control (Fig. 7) at 380 ^{o}C.

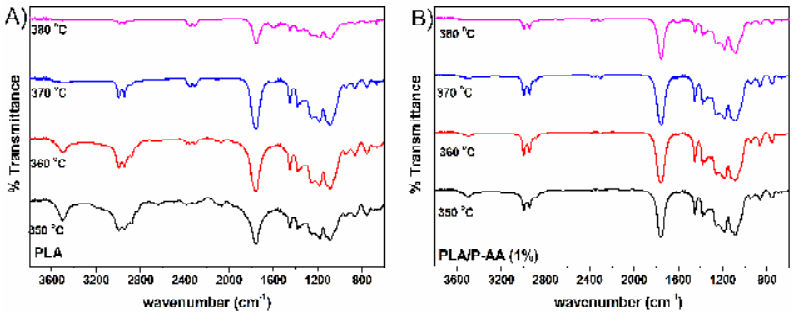

Fig. 7 A) FTIR spectra of solid phase during thermal decomposition of PLA at different temperature; B) the FTIR spectra of solid phase during thermal decomposition of PLA/P-AA (1%) at different temperature

Tensile properties

Tensile property is one of most important mechanical properties for PLA. Fig. 8 A) described the stress-stain curves of PLA and PLA/P-AA composites. Fig. 8 B) listed the plot of tensile strength and Young's modulus against P-AA loading. PLA control showed typical brittle fracture without yielding during the test as shown in Fig. 8 A). When P-AA was added in to PLA, PLA/P-AA still showed the brittle fracture without yield. From Fig. 8 B), the tensile strength and Young's modulus of PLA fluctuated slightly within 1 wt%, which was considered to be negligible. On view of molecular structure, P-AA was homogenously mixed with PLA. The addition of P-AA might induce plasticization and

some impacts on crystallization of PLA. However, the small loading of P-AA did not show these effects in apparent way.

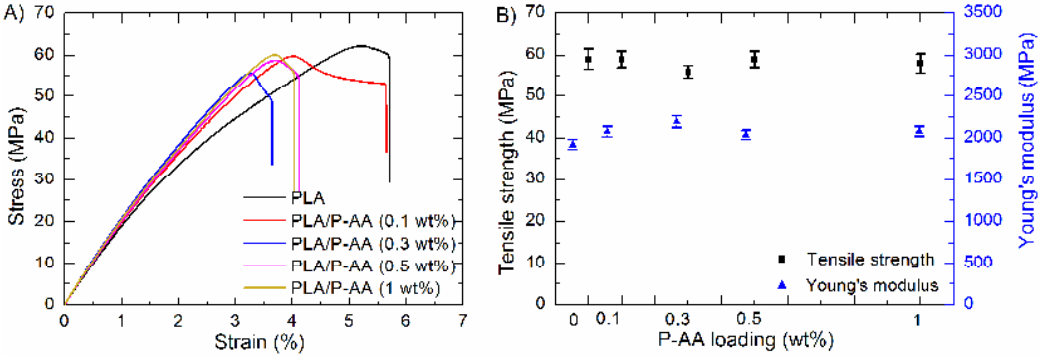

Fig. 8 A) Stress-strain curves of PLA and PLA/P-AA composites; B) the plots of tensile strength and Young's modulus against loading of P-AA

Conclusion

In this work, flame retardant P-AA exhibited super efficiency on reducing the flammability of PLA. Only 0.5 wt% loading of P-AA increased LOI value of PLA from 20.5 to 28.4 and passed UL 94 V-0 rating at 3.2 mm thickness. As the loading of P-AA increased to 1 wt%, flame-retardant PLA even passed UL 94 V-0 rating at 1.6 mm thickness. Special phenomena on the surface temperature during UL 94 test had been discovered, showing that the surface temperature of PLA control continuously increased during the 1st 10 s ignition, whereas that of PLA/P-AA (0.5 wt%) first increased until 5-7 seconds, afterwards the temperature decreased. Furthermore, the addition of P-AA changed the combustion behaviour of PLA. PLA/P-AA (0.5 or 1 wt%) showed a lower pHRR compared with PLA control. TTI of PLA/P-AA (1 wt%) prolonged to 111 (±5) s which was 45 s longer than that of PLA. Flame inhibition caused by PO· radicals from the thermal decomposition of P-AA was considered to be the main mechanism to induce the high improvements on flame retardancy of PLA. Based on the study of thermal decomposition behaviour, it concluded that the addition of P-AA slightly decreased the apparent activation energy (Ea) of PLA, clearly dropped peak intensity at 1244 cm^{-1} in the evolved gaseous products. Moreover, in comparison to PLA control, tensile properties of PLA/P-AA kept at the same level after the small loading amount of P-AA.

Supporting Information

The NMR spectra and FTIR spectra of P-AA (Figures S1-S4)

Videos of UL 94 tests for PLA and PLA/P-AA (1 wt%) with 3.2 and 1.6 mm thickness

This material is available free of charge via the Internet at http://pubs.acs.org

Author Information

Corresponding Author

*Tel: 0034-91-5493422-1055; fax: 0034-91-5503047; e-mail: deyi.wang@imdea.org

Notes

The authors declare no competing financial interest.

Acknowledgement

This research is funded by Spanish Ministry of Economy and Competitiveness (MINECO) under Ramón y Cajal grant (RYC-2012-10737). Also, one of our authors (Ms. Xiaomin Zhao) would thank the financial support from China Scholarship Council.

References

(1). Auras, R. A.; Lim, L.-T.; Selke, S. E.; & Tsuji, H. *Poly (lactic acid): synthesis, structures, properties, processing, and applications*. John Wiley & Sons, 2011.

(2). Sin, L. T.; Rahmat, A. R.; & Rahman, W. A. *Polylactic acid: PLA biopolymer technology and applications*. **2012,** William Andrew.

(3). Bourbigot, S.; & Fontaine, G. Flame retardancy of polylactide: an overview. *Polymer Chemistry* . **2010**, *1*(9), 1413-1422.

(4). Song, Y.P.; Wang, D.Y.; Wang, X.L.; Lin, L.; & Wang, Y.Z. A method for simultaneously improving the flame retardancy and toughness of PLA. *Polymer for Advanced Technologies*, **2011**, 22 2295-2301.

(5). Chow, W. S.; & Teoh, E. L. Flexible and Flame Resistant Poly(lactic acid)/Organomontmorillonite Nanocomposites. *J. Appl. Polym. Sci.* **2015,** *132*(2).

(6). Wei, L.L.; Wang, D.Y.; Chen H.B.; Chen, L.; Wang, X.L.; & Wang, Y.Z. Effect of phosphorus-containing flame retardant on the thermal and early flaming behaviors of poly(lactic acid) *Polym. Degrad. Stab.* **2011**, 96(9): 1557-1561

(7). Liu, X.Q.; Wang, D.Y.; Wang, X.L.; Chen, L.; & Wang, Y.Z. Synthesis organo-modified α-Zirconium phosphate and its effect on the flame retardancy of IFR poly (lactic acid) systems. *Polym. Degrad. Stab.***2011**, 96(5): 771-777

(8). Yuan, X.Y.; Wang, D.Y.; Chen, L.; Wang, X.L.; & Wang, Y.Z. Inherent flame retardation of bio-based poly(lactic acid) by incorporating phosphorus linked pendent group into the backbone. *Polym. Degrad. Stab.* **2011**, 96, 1669-1675.

(9). Mauldin, T. C.; Zammarano, M.; Gilman, J. W.; Shields, J. R.; & Boday, D. J. Synthesis and characterization of isosorbide-based polyphosphonates as biobased flame-retardants. *Polymer Chemistry*. **2014**, *5*(17), 5139-5146.

(10). Murariu, M.; Bonnaud, L.; Yoann, P.; Fontaine, G.; Bourbigot, S.; & Dubois, P. (**2010**). New trends in polylactide (PLA)-based materials:"Green" PLA–Calcium sulfate (nano) composites tailored with flame retardant properties. *Polym. Degrad. Stab.*. *95*(3), 374-381.

(11). Akbari, A.; Majumder, M.; & Tehrani, A. Polylactic Acid (PLA) Carbon Nanotube Nanocomposites. *Handbook of Polymer Nanocomposites. Processing, Performance and Application*; Springer, 2015.

(12). Fox, D. M.; Novy, M.; Brown, K.; Zammarano, M.; Harris, R. H.; Jr.; Murariu, M.; McCarthy, E. D.; Seppala, J. E.; & Gilman, J. W. Flame retarded poly(lactic acid) using PUSS-modified cellulose. 2. Effects of intumescing flame retardant formulations on polymer degradation and composite physical properties. *Polym. Degrad. Stab.* . **2014,** *106*, 54-62.

(13). Gao, Y.; Wu, J.; Wang, Q.; Wilkie, C. A.; & O'Hare, D. Flame retardant polymer/layered double hydroxide nanocomposites. *J. Mater. Chem. A.* **2014,** *2*(29), 10996-11016.

(14). Bocz, K.; Domonkos, M.; Igricz, T.; Kmetty, A.; Barany, T.; & Marosi, G. Flame retarded self-reinforced poly(lactic acid) composites of outstanding impact resistance. *Compos Part A: Appl Sci Manufac.*. **2015**, *70*, 27-34.

(15). Stoclet, G.; Sclavons, M.; Lecouvet, B.; Devaux, J.; Van Velthem, P.; Boborodea, A.; Bourbigot, S.; & Sallem-Idrissi, N. Elaboration of poly (lactic acid)/halloysite nanocomposites by means of water assisted extrusion: structure, mechanical properties and fire performance. *RSC Advances.* **2014,** *4*(101), 57553-57563.

(16). Song, L.; Xuan, S.; Wang, X.; & Hu, Y. Flame retardancy and thermal degradation behaviors of phosphate in combination with POSS in polylactide composites. *Thermochimi Acta* .**2012,** *527*, 1-7.

(17). Wei, P.; Bocchini, S.; & Camino, G. Nanocomposites combustion peculiarities. A case history: Polylactide-clays. *Eur. Polym. J.*. **2013,** *49*(4), 932-939.

(18). Qian, Y.; Wei, P.; Jiang, P.; Li, Z.; Yan, Y.; & Ji, K. Aluminated mesoporous silica as novel high-effective flame retardant in polylactide. *Compos. Sci. Technol.*. **2013,** *82*, 1-7.

(19). Wang, D.-Y.; Song, Y.-P.; Lin, L.; Wang, X.-L.; & Wang, Y.-Z. A novel phosphorus-containing poly (lactic acid) toward its flame retardation. *Polymer.* **2011,** *52*(2), 233-238.

(20). Zhao，X.M.; Llorca, J.; & Wang, D.-Y. Novel approach to fire-retardant polymeric material based on epoxy by tunable phosphorus "chemical surrounding". **2015 (submitted)**.

(21). Brown, M.; Maciejewski, M.; Vyazovkin, S.; Nomen, R.; Sempere, J.; Burnham, A. a.; Opfermann, J.; Strey, R.; Anderson, H.; & Kemmler, A. Computational aspects of kinetic analysis: part A: the ICTAC kinetics project-data, methods and results. *Thermochim Acta.* **2000**, *355*(1), 125-143.

(22). Yao, F.; Wu, Q.; Lei, Y.; Guo, W.; & Xu, Y. Thermal decomposition kinetics of natural fibers: activation energy with dynamic thermogravimetric analysis. *Polym. Degrad. Stab.*.**2008,** *93*(1), 90-98.

(23). Zou, H.; Yi, C.; Wang, L.; Liu, H.; & Xu, W. Thermal degradation of poly (lactic acid) measured by thermogravimetry coupled to Fourier transform infrared spectroscopy. *J. Therm. Anal. Calorim.*. **2009**, *97*(3), 929-935.

(24). Kopinke, F.-D.; Remmler, M.; Mackenzie, K.; Möder, M.; & Wachsen, O. Thermal decomposition of biodegradable polyesters—II. Poly (lactic acid). *Polym. Degrad. Stab.*. **1996***, 53*(3), 329-342.

Figure captions

Scheme 1 The synthesis rout of flame retardant P-AA

Fig. 1 A) The screenshots from UL 94 test videos of PLA with thickness 1.6 and 3.2 mm, PLA/P-AA (1 wt%) with thickness 1.6 mm and PLA/P-AA (0.5 wt%) with thickness 3.2 mm; B) the surface temperature monitored by IR thermometer vs time curves of PLA and PLA/P-AA (0.5 wt%) (3.2 mm)

Fig. 2 A) HRR vs time curves of PLA and PLA/P-AA; B) mass curves of PLA and PLA/P-AA

Fig. 3 TGA and DTG curves of PLA and PLA/P-AA composites

Fig. 4 A) The plot curves of ln (β/T^2) against 1/T of PLA at different α; B) The plot curves of ln (β/T^2) against 1/T of PLA/P-AA (1 wt%) at different α

Fig.5 A) 3-D image of TGA-FTIR results of PLA; B) the 3-D image of TGA-FTIR results of PLA/P-AA (1 wt%); C) the Gram- Schmidt curves vs temperature of PLA and PLA/P-AA (1wt%); D) the absorbance at 1244 cm^{-1} vs temperature curves of PLA and PLA/P-AA (1wt%);

Fig. 6 FTIR spectra of evolved gas products of PLA around 380 ^oC

Fig. 7 A) FTIR spectra of solid phase during thermal decompositionof PLA at different temperature; B) the FTIR spectra of solid phase during thermal decompositionof PLA/P-AA (1%) at different temperature

Fig. 8 A) Stress-strain curves of PLA and PLA/P-AA composites; B) the plots of tensile strength and Young's modulus against loading of P-AA

Table captions

Tab. 1 LOI and UL 94 results of PLA and PLA/P-AA composites

Tab. 2 CONE data for PLA and PLA/P-AA at 35 kW/m^2

Tab. 3 Calculated Ea and r^2 of PLA and PLA/P-AA (1 wt%) at different decomposition α

Table of Contents

A new super-efficiently flame-retardant bioplastic-poly (lactic acid): flammability, thermal decomposition behavior and tensile properties

Xiaomin Zhao[1,2], Francisco Reyes Guerrero[1], Javier Llorca[1,2], De-Yi Wang[1]*

[1]IMDEA Materials Institute, C/Eric Kandel, 2, 28906 Getafe, Madrid, Spain

[2]Technical University of Madrid (UPM), 28006, Madrid, Spain

Corresponding author: De-Yi Wang: Tel.: +34-917871888, *E-mail address*: deyi.wang@imdea.org

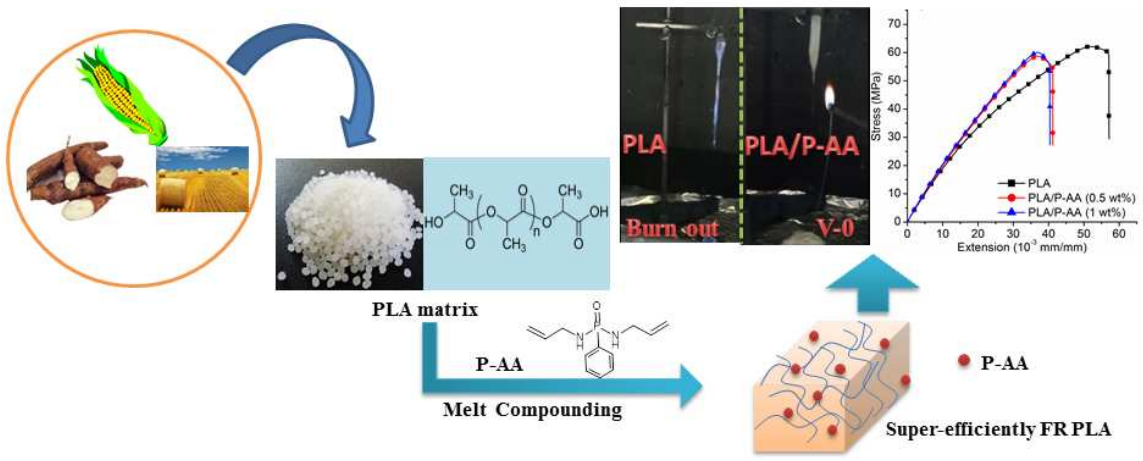

SYNOPSYS: A super-efficiently flame-retardant bioplastic-polylactic acid (PLA) shows extremely high flame retardancy and maintains the tensile property at the same level.